

See discussions, stats, and author profiles for this publication at: <https://www.researchgate.net/publication/7844593>

AAS, XRPD, SEM/EDS, and FTIR characterization of Zn²⁺ retention by calcite, calcite-kaolinite, and calcite-clinoptilolite minerals

Article *in* Journal of Colloid and Interface Science · June 2005

DOI: 10.1016/j.jcis.2005.02.047 · Source: PubMed

CITATIONS

26

READS

31

4 authors, including:



Talal Shahwan

Birzeit University

54 PUBLICATIONS 1,293 CITATIONS

SEE PROFILE

AAS, XRPD, SEM/EDS, and FTIR characterization of Zn^{2+} retention by calcite, calcite–kaolinite, and calcite–clinoptilolite minerals

T. Shahwan*, B. Zünbül, Ö. Tunusoğlu, A.E. Eroğlu

Department of Chemistry, Izmir Institute of Technology, Urla 35430, İzmir, Turkey

Received 8 November 2004; accepted 3 February 2005

Available online 8 April 2005

Abstract

In this study, the sorption behavior of Zn^{2+} on calcite, kaolinite, and clinoptilolite, in addition to mixtures of calcite with kaolinite and clinoptilolite, was investigated at various loadings and mixture compositions using atomic absorption spectroscopy, scanning electron microscopy/energy dispersive X-ray spectroscopy, X-ray powder diffraction, and Fourier transform infrared techniques. According to the obtained results, within the experimental operating conditions, the sorption capacity was enhanced with increasing amount of calcite in both types of mixtures. Under neutral–alkaline pH conditions and high loadings, the order of Zn^{2+} retention was observed as calcite > clinoptilolite > kaolinite. The experiments on the retention of Zn^{2+} by pure calcite under conditions of oversaturation showed that the uptake process proceeds via an initial adsorption mechanism (possibly ion-exchange type) followed by a slower mechanism that leads to the overgrowth of the hydrozincite phase, $Zn_5(OH)_6(CO_3)_2$.

© 2005 Elsevier Inc. All rights reserved.

Keywords: Zinc; Kaolinite; Clinoptilolite; Calcite; Hydrozincite

1. Introduction

In the geochemical environment, reactions taking place at the interface between aqueous media and soil fractions are important in regulating the transport of chemical species through the hydrosphere. Radionuclides produced by fission or activation processes in nuclear facilities are considered to form detriment to the biological environment unless their migration is delayed or retarded by manmade or natural barriers. Zn possesses the radioactive isotope, ^{65}Zn ($t_{1/2} = 244$ days), which is produced by nuclear activation reactions. Moreover, the risk of Zn phytotoxicity in soils has increased in various regions following application of different anthropogenic materials [1].

Kaolinite, clinoptilolite, and calcite are important examples of minerals that are intensively present as soil components. Kaolinite, $Al_2Si_2O_5(OH)_4$, is one of the most widely

available clay minerals, which are well known for their layered structure. Clinoptilolite, $(Na,K)_6Al_6(Si_{30}O_{72}) \cdot 20H_2O$, is the most abundant zeolite type in nature that possesses a heulandite (HEU) type framework with a network of channels that are predominantly occupied by Na, K, Ca, and H_2O . Calcite is the most stable polymorph of $CaCO_3$, a mineral that is frequently associated with other soil components. This association affects the uptake properties of these minerals in terms of their sorption capacities as well as their sorption mechanisms, particularly, in alkaline media. From the radioactive waste management viewpoint, this would be important, as the degradation of concrete in the disposal facilities is expected to release high pH [2].

Lots of studies exist in the literature in which investigations of different aspects of the sorption behavior of Zn^{2+} on the individual minerals of kaolinite, clinoptilolite, and calcite were reported [3–9]. However, our literature survey revealed only a limited number of studies, which have so far been devoted to studying the effect of calcite content on the sorption characteristics of various types of soil fractions toward Zn^{2+} ions [10–13]. These studies provided important

* Corresponding author. Fax: +90-232-750-7509.

E-mail address: talalshahwan@iyte.edu.tr (T. Shahwan).

information regarding various aspects of Zn^{2+} interaction and generally reported a positive correlation between the amount of removed Zn^{2+} ions and that of calcite or CaCO_3 in different types of calcareous soils. However, to our knowledge, no literature resources have addressed the topic of this work.

This study presented is part of ongoing research in which the sorption behavior of various metals on mixtures of calcite or magnesite with natural kaolinite and clinoptilolite is investigated. In this particular study, the uptake of Zn by calcite, clinoptilolite, kaolinite, and calcite–kaolinite and calcite–clinoptilolite mixtures is discussed in terms of the sorbed quantities and plausible mechanisms of sorption. Flame atomic absorption spectroscopy (AAS) was applied for the determination of the bulk concentrations of Zn^{2+} . X-ray powder diffraction (XRPD) was used to reveal the structural changes associated with the sorption process. The morphology of the minerals was analyzed using scanning electron microscopy (SEM), and the elemental composition was revealed using energy dispersive X-ray spectroscopy (EDS). Infrared spectroscopy (FTIR) was used to analyze the effect of Zn^{2+} incorporation on the vibrational bands of calcite and reveal the bands corresponding to the precipitated Zn compound(s).

2. Experimental

The natural samples kaolinite and clinoptilolite applied in this work were dry-sieved, and the particle size of applied kaolinite was 38–75 μm while that of clinoptilolite was 75–150 μm . The particle size of calcite (CaCO_3 ; Carloerba) used throughout this study was 48–600 μm . The experiments were performed using 50-ml polyethylene tubes. To each tube, 0.50 g of the solid mixture were added, followed by the addition of 50 ml of aqueous $\text{Zn}(\text{NO}_3)_2$ solution. The concentration of the solutions were 1, 100, 500, 3000, and 10,000 mg/L. The solid mixtures were prepared by mixing appropriate amounts of CaCO_3 with kaolinite or clinoptilolite to yield percentage compositions of 5, 10, 25, and 60% CaCO_3 . The initial (at the start of mixing) and final (at the end of mixing) pH values of the mixtures are given in Table 1. In freshwater media, up to neutral pH conditions, the chemical form of zinc is predominantly Zn^{2+} ions. As the pH increases beyond ~ 7 , the hydroxy ions, e.g., ZnOH^+ ,

start to compete with the Zn^{2+} ions [14]. As seen from the pH values given by Table 1, when the initial concentration of zinc ions is increased, the pH decreases, indicating that at high concentrations the prevailing chemical form of zinc is Zn^{2+} .

All the experiments were conducted using the batch method at 25 °C under atmospheric pressure and were mixed for 48 h. A Nüve (Ankara, Turkey) ST 402 water bath shaker equipped with a microprocessor thermostat was used for mixing. At the end of each mixing period, the samples were filtered and dried at 90 °C. The filtrates were then analyzed using flame AAS using a Thermo Elemental SOLAAR M6 Series atomic absorption spectrometer with air–acetylene flame. Zn hollow cathode lamp ($\lambda = 213.9 \text{ nm}$) was applied as source.

The XRPD analysis of the powders was performed using a Philips X'Pert Pro diffractometer. The samples were first ground and mounted on Si holders and then introduced for analysis. The source consisted of $\text{CuK}\alpha$ radiation ($\lambda = 1.54 \text{ \AA}$). Each sample was scanned with a step size of 0.020 in the 2θ range of 2–60.

SEM/EDS characterization was carried out using a Philips XL-30S FEG type instrument. The solid samples were sprinkled onto adhesive carbon tapes supported on metallic disks and introduced for analysis. Images of the sample surfaces were recorded at various magnifications. Spot EDS elemental analysis was performed at different points on the surface in order to minimize any possible anomalies arising from the heterogeneous nature of the analyzed surface.

3. Results and discussion

XRPD characterization of the minerals (see Fig. 1) prior to sorption indicated that while clinoptilolite was almost pure, natural kaolinite fractions contained quartz as an impurity. Similar characterization of CaCO_3 validated that the mineral is entirely composed of calcite. The EDS results (atomic percentages) showed that the average elemental content of kaolinite was 66.8% O, 17.6% Si, and 14.1% Al, together with minor quantities of Na, K, Mg, and Ca. The average elemental composition of clinoptilolite was 61.9% O, 23.7% Si, and 5.3% Al, with small amounts of Na, K, Mg, and Ca. The average atomic content of calcite was 28.4% C, 50.9% O, and 20.7% Ca. The given EDS values represent an average of five data points obtained from random locations on the mineral surface. SEM characterization showed that kaolinite has a well-defined crystal structure, revealed by its typical hexagonal plates with edge sizes ranging from 300 to 500 nm. Clinoptilolite, however, seems to be composed of crystals with varying sizes that amount to several micrometers. SEM characterization of calcite showed that the mineral is mostly formed of aggregates with variable shapes and sizes.

The sorption behavior of Zn^{2+} was first investigated on the individual minerals of kaolinite, clinoptilolite, and calcite. The partition of Zn^{2+} among solid and liquid phases

Table 1
Initial (minimum) and final (maximum) pH values of the $\text{Zn}(\text{NO}_3)_2$ solutions in contact with various calcite–kaolinite and calcite–clinoptilolite mixtures

Initial concentration (mg/L)	Initial–final pH of solution	
	Calcite–kaolinite	Calcite–clinoptilolite
1	9.1–9.2	9.6–9.4
100	7.1–8.3	7.3–8.7
500	7.0–7.3	7.1–7.8
3000	5.9–6.5	5.5–6.6
10,000	5.4–5.9	5.7–6.0

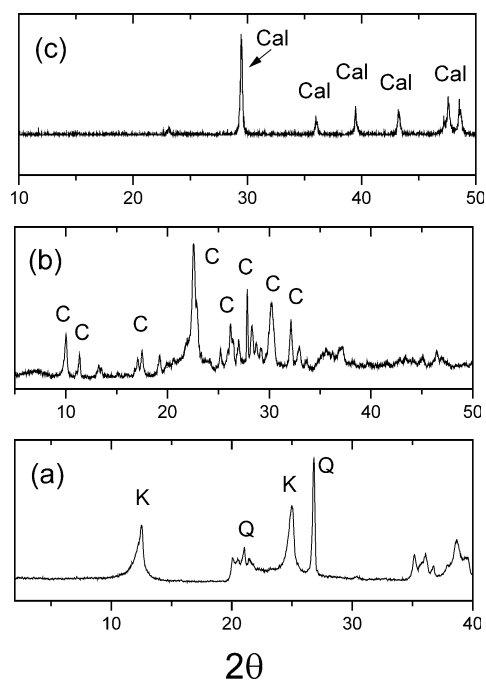


Fig. 1. XRPD patterns of the minerals used in this study, kaolinite (a), clinoptilolite (b), and calcite (c).

upon sorption was characterized using Langmuir and Freundlich sorption isotherms. The two isotherms are widely used because they are convenient to describe experimental results over a wide range of concentrations [7]. Langmuir isotherm is given by the equation

$$[C]_s = \frac{bC_m[C]_i}{1 + b[C]_i}, \quad (1)$$

where $[C]_s$ is the equilibrium amount of solute per unit mass of solid phase (mg/g), $[C]_i$ is the equilibrium concentration of sorbate in solution (mg/L), C_m is the maximum amount of sorbate that can be sorbed by solid phase (mg/g), and b is a constant related to the energy of sorption. This sorption model did not adequately describe the sorption data of Zn^{2+} on each of the three minerals. This could stem from the fact that Langmuir sorption isotherm is valid for sorption on homogeneous solids with a monolayer coverage in which the sorbed species do not interact with each other. Alternatively, the Freundlich isotherm model is given by the equation

$$[C]_s = k[C]_i^n. \quad (2)$$

Here, $[C]_s$ and $[C]_i$ are as defined above, k and n are Freundlich constants that refer to sorption capacity and linearity of sorption, respectively. This model was seen to better describe the sorption data compared with Langmuir model. Freundlich isotherm is suitable for description of sorption taking place on heterogeneous solids where multilayer sorption is allowed. The plots constructed utilizing Freundlich model for sorption of Zn^{2+} ions on kaolinite, clinoptilolite, and calcite are shown in Fig. 2. The values of n and k obtained from the slope and intercept of the plots of $\log[C]_s$ against $\log[C]_i$ are provided in Table 2. The values

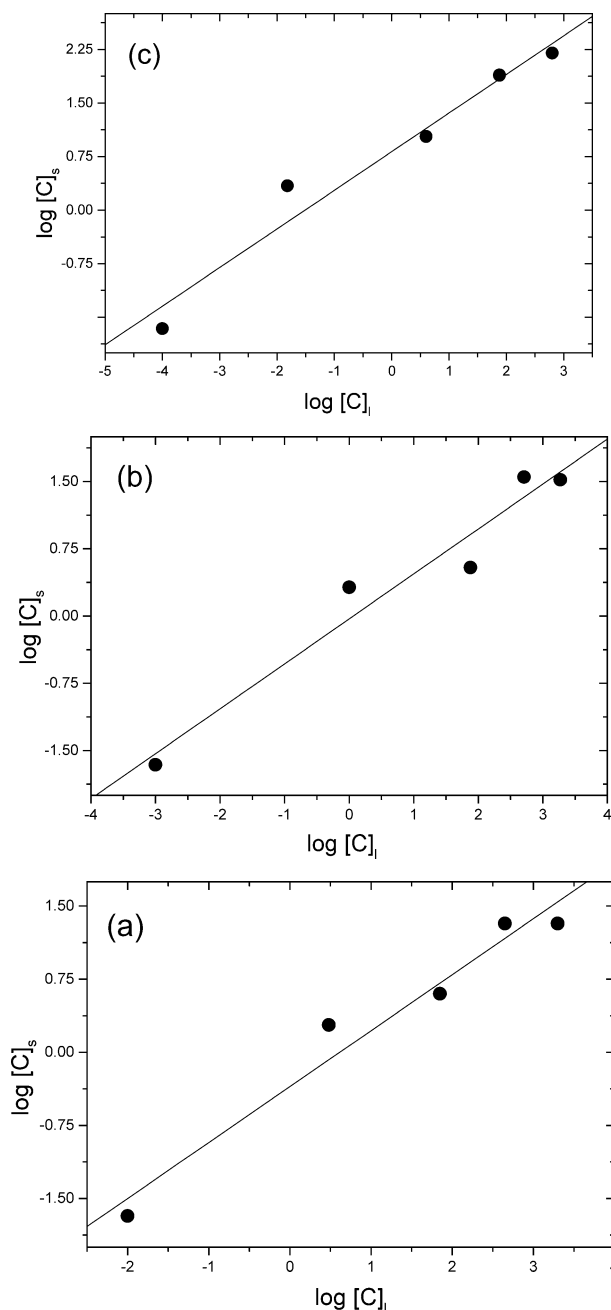


Fig. 2. Freundlich isotherm plots for sorption of Zn^{2+} on (a) kaolinite, (b) clinoptilolite, and (c) calcite.

of n being less than 1.0 indicate that sorption is nonlinear in all cases and suggest a progressive decrease in the fixation ability of the solids as the initial concentration of Zn^{2+} is increased. According to the k values, the sorption capacity of the solids follows the order calcite > clinoptilolite > kaolinite, with that of calcite being prominently larger than the corresponding values of clinoptilolite and kaolinite. This observation is also verified from the values of percentage sorption calculated using the equation

$$PS = \frac{[C]_0 - [C]_i}{[C]_0} \times 100\%. \quad (3)$$

Table 2

Values of Freundlich constants n and k corresponding to sorption of Zn^{2+} on kaolinite, clinoptilolite, and calcite

	n	k (mg/g)	R
Zn–kaolinite	0.57	0.44	0.9797
Zn–clinoptilolite	0.50	0.93	0.9752
Zn–calcite	0.53	6.76	0.9792

Note. The linear correlation coefficients, R , are also provided.

In this equation PS refers to percentage sorption, $[C]_1$ is as defined above, and $[C]_0$ stands for the initial concentration. The calculated values of percentage sorption of Zn^{2+} on kaolinite, clinoptilolite, and calcite are provided in Table 3 (part I). It is interesting to see that the percentage sorption of calcite at the highest studied concentration (10,000 mg/L $Zn(NO_3)_2$) exceeds that of pure kaolinite by sevenfold, and that of pure clinoptilolite by more than fourfold. As was described in the experimental parts, the uptake of Zn^{2+} was also investigated on mixtures of calcite with kaolinite and with clinoptilolite at various compositions. The results obtained from the sorption experiments on calcite–kaolinite and calcite–clinoptilolite mixtures, given in Table 3 (parts II and III), indicated an increased amount of scavenged Zn^{2+} ions with the increased fraction of calcite in the mixtures. Comparing parts I, II, and III in the table, it is clear that the three individual minerals are capable to scavenge Zn^{2+} ions almost totally at concentrations lower than 100 mg/L. As the initial concentration is increased beyond this value, the efficiency of removal of kaolinite and clinoptilolite minerals decreases largely and the presence of calcite in the mixtures of kaolinite and clinoptilolite starts

Table 3

The values of percentage sorption of Zn^{2+} on individual kaolinite, clinoptilolite, and calcite minerals, in addition to calcite–kaolinite and calcite–clinoptilolite mixtures

I. % Sorption on individual minerals

Initial concentration (mg/L)	Kaolinite	Clinoptilolite	Calcite
1	>99.9	>99.9	>99.9
100	86.4	95.5	>99.9
500	36.4	31.8	96.4
3000	31.8	22.9	88.6
10,000	9.5	15.0	71.6

II. % Sorption on calcite–kaolinite mixtures

Initial concentration (mg/L)	5% Calcite	10% Calcite	25% Calcite	60% Calcite
1	>99.9	>99.9	>99.9	>99.9
100	>99.9	>99.9	>99.9	>99.9
500	60.0	77.3	93.6	97.3
3000	48.0	45.5	51.1	79.7
10,000	10.1	10.9	37.0	42.0

III. % Sorption on calcite–clinoptilolite mixtures

Initial concentration (mg/L)	5% Calcite	10% Calcite	25% Calcite	60% Calcite
1	>99.9	>99.9	>99.9	>99.9
100	>99.9	>99.9	>99.9	>99.9
500	72.7	92.7	95.5	98.2
3000	47.0	48.6	61.5	86.4
10,000	16.1	33.6	66.8	67.7

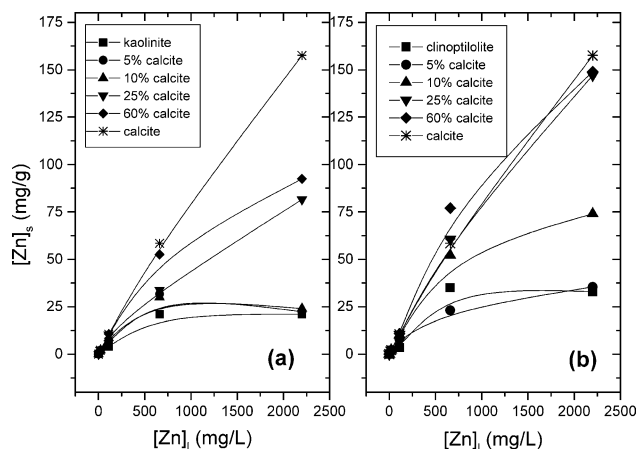


Fig. 3. Variation of the equilibrium concentration on the solid phase with that in the liquid phase for different Zn^{2+} loadings and mixture compositions: (a) calcite–kaolinite, (b) calcite–clinoptilolite.

to enhance the fixation capacity of the solid mixture. Consequently, within the studied experimental conditions, calcite stands as the most significant sink for zinc among these three minerals.

The variation of the sorbed amounts of Zn^{2+} ions with their equilibrium liquid concentrations on calcite–kaolinite and calcite–clinoptilolite mixtures is given in Fig. 3. The saturation in the amount of retarded Zn^{2+} observed when pure kaolinite or clinoptilolite are used appears to vanish as the mixtures become richer in calcite. This is more pronounced in the case of calcite–kaolinite mixtures due to the larger difference in the sorption capacities between kaolinite and calcite.

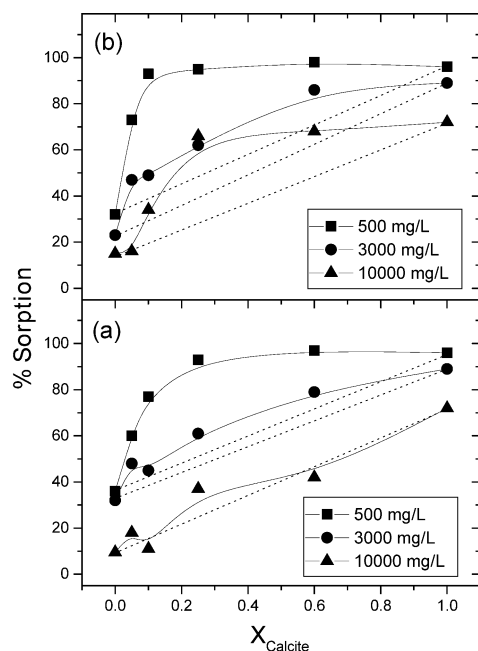


Fig. 4. The change of percentage sorption with the fraction of calcite at initial loadings of 500, 3000, and 10,000 mg/L of $\text{Zn}(\text{NO}_3)_2$: (a) calcite–kaolinite, (b) calcite–clinoptilolite.

If the mixtures were behaving ideally, then the total percentage sorption would be predicted using the equation

$$\text{PS} = \frac{m_A}{m_A + m_B} (\text{PS})_A + \frac{m_B}{m_A + m_B} (\text{PS})_B, \quad (4)$$

where m_A and m_B are the masses of components A and B in their solid mixture. The variation of percentage sorption obtained for the initial concentrations of 500, 3000, and 10,000 mg/L of $\text{Zn}(\text{NO}_3)_2$ is plotted as a function of calcite fraction in the mixtures as given by Fig. 4. The same figure also provides the values predicted by Eq. (4) (dotted lines). The figure suggests an increase in the percentage sorption of Zn^{2+} as the fraction of calcite in the mixtures is increased and at the initial concentration of 500 mg/L, the curves are shown to form a plateau corresponding to almost total removal of Zn^{2+} ions even at calcite content of less than 50%. As implied by the figure, when the initial concentration is increased to 3000 and 10,000 mg/L, more calcite is required to enhance the removal of Zn. It can also be noticed that in the case of calcite–kaolinite mixtures, as the initial concentration of Zn solution is increased to 10,000 mg/L, the experimental values of percentage sorption become closer to those predicted by Eq. (4). This is merely stemming from the fact that at higher loading, kaolinite becomes inefficient in sorption which is in turn predominantly controlled by calcite, so that Eq. (4) can be approximated as

$$\text{PS} \cong \frac{m_{\text{calcite}}}{m_{\text{calcite}} + m_{\text{kaolinite}}} (\text{PS})_{\text{calcite}}. \quad (5)$$

The XRPD analysis of the Zn-loaded solids showed no changes in the structures of kaolinite and clinoptilolite. In both minerals, unless the pH conditions are very acidic,

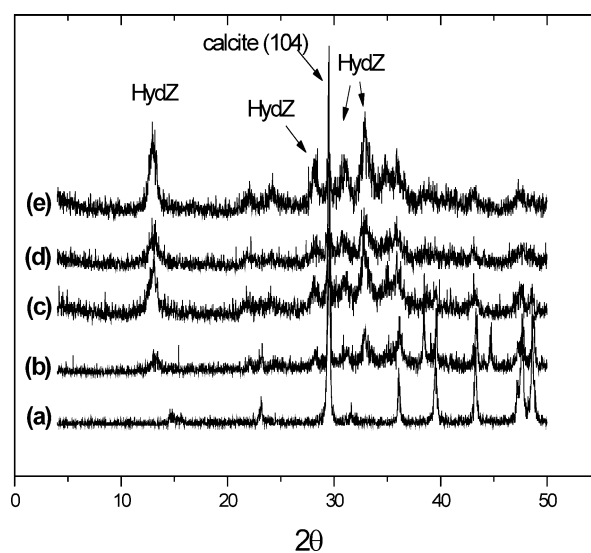


Fig. 5. XRPD diagrams of Zn-loaded calcite, showing the formation of hydrozincite at different contact times, initially (a) and after 7 h (b), 24 h (c), 48 h (d), and 7 days (e).

no matrix changes are expected to accompany the sorption process. These findings were also verified from the SEM images, which showed no change in the morphology and crystal size of the two Zn-loaded minerals. Due to its prominent performance in Zn removal, more consideration was given to calcite fractions in the further experiments.

The sorption mechanism on the calcite fractions can plausibly occur via various processes: ion exchange, burial of the ions within the lattice of carbonate upon recrystallization, formation of surface complexes with $>\text{CaOH}$ and $>\text{CO}_3\text{H}$ groups, precipitation as metal carbonate, metal hydroxide, or both, and solid state diffusion [15]. Our XRPD results indicated that, up to an initial concentration of 3000 mg/L of $\text{Zn}(\text{NO}_3)_2$, no overgrowth of any precipitate (zinc carbonate/hydroxide species) was observed. Thus, up to this concentration, the sorption mechanism of Zn^{2+} ions is plausibly ion exchange and/or incorporation at the cavities of calcite surface, in addition to the possibility of complexation with the exposed surface $>\text{CaOH}$ groups, especially at lower concentration where the pH was high enough to justify the formation of such hydroxyl groups at calcite surface. Beyond this concentration, formation of hydrozincite ($\text{Zn}_5(\text{OH})_6(\text{CO}_3)_2$) was detected in the samples containing initially a calcite weight fraction of 0.60 in addition to pure calcite. This precipitate formation was detected in spite of the fact the pH of the medium was slightly acidic at the concentrations of 3000 and 10,000 mg/L (see Table 1). In a separate experiment, the initial pH of the reaction medium was raised to 10.0, for the initial concentrations of 3000 and 10,000 mg/L, to check its effect on the identity of the precipitate. The XRPD and SEM results indicated the formation of the same particles, i.e., hydrozincite, but in a more massive fashion, indicating an increased uptake of zinc in the form of hydrozincite possibly due to the higher availability of carbonate and hydroxide ions at pH 10.0. Hydrozincite

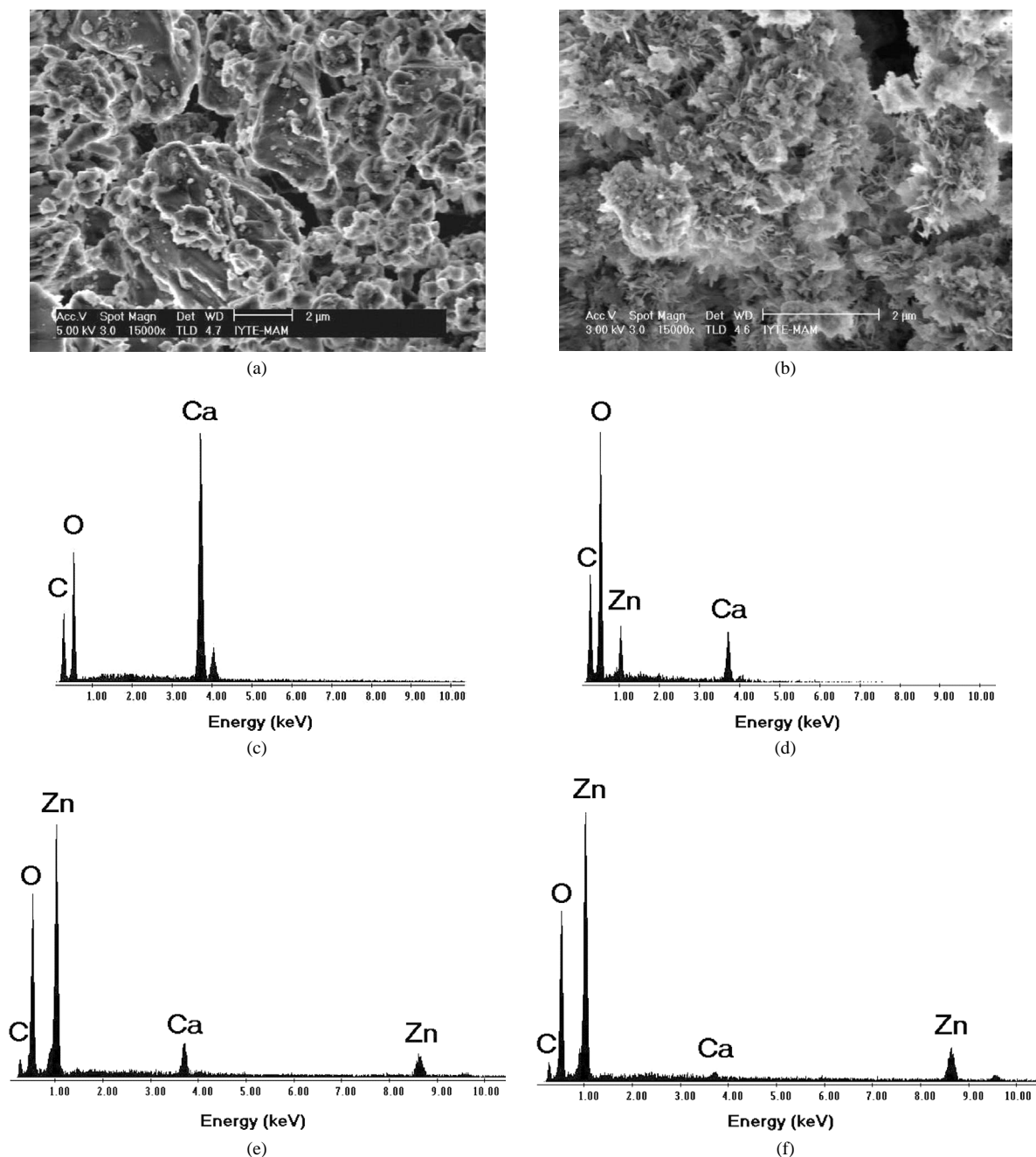


Fig. 6. Typical SEM micrographs of calcite (a), and hydrozincite (b). EDS spectra of Zn-loaded calcite at different contact times: initially (c) and after 1 h (d), 24 h (e), and 3 weeks (f).

formation was also previously reported as the uptake mechanism of Zn^{2+} by calcite [16]. In another study, formation of hydrozincite crystals was documented along with the formation of minor composite phases corresponding to the rare mineral minrecordite, $\text{CaZn}(\text{CO}_3)_2$ [17]. On the contrary, based on an EXAFS study, the formation of hydrozincite was not documented upon Zn–calcite interaction [8].

It seems that the formation of hydrozincite, rather than zincite, at high Zn^{2+} loadings does not have much to do with the formation of ZnOH^+ as a speciation product since, at such loadings, the pH of the reaction medium was measured

to be $\sim 6\text{--}7$ (see Table 1), where the chemical speciation of zinc is expected to be dominated by Zn^{2+} . Moreover, our ongoing kinetic studies on overgrowth of precipitates of various ions contacted with pure calcite and carried out over long mixing period (3–4 weeks), indicated that formation of zinc carbonate species occurs slower than that of other ions like Ba^{2+} , Sr^{2+} , and Pb^{2+} . According to our results, while precipitate overgrowth of these ions occurs and levels up within a time scale of hours, that corresponding to Zn^{2+} takes a time period ranging from days to weeks depending on the experimental conditions, in particular, loading and pH. Fig. 5

Table 4

The atomic percentages of C, O, Ca, and Zn in calcite structure before sorption, and after different sorption periods

Element	Calcite	Zn–calcite (1 h)	Zn–calcite (2 h)	Zn–calcite (24 h)	Zn–calcite (1 week)
C K	28.4	29.6	31.2	21.6	22.4
O K	50.9	49.2	47.1	54.9	55.2
Ca K	20.7	18.8	14.6	3.8	1.1
Zn L	0	2.4	7.1	19.7	21.3
Total	100	100	100	100	100

Note. The data are based on EDS measurements.

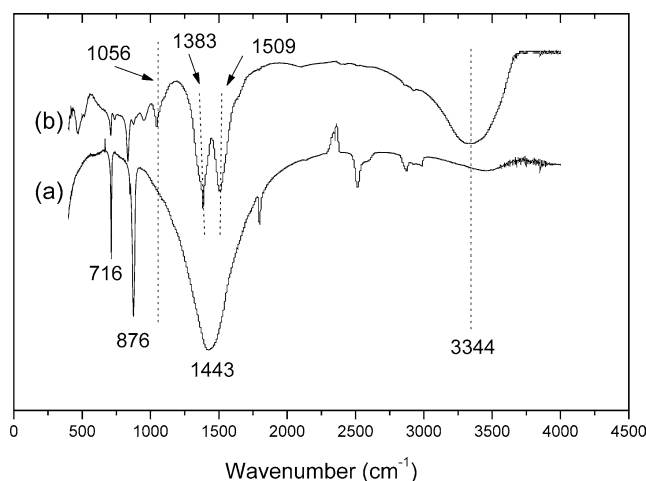


Fig. 7. FTIR spectra of calcite (a) and Zn-loaded calcite after 7 days of contact (b).

gives the XRPD patterns of Zn-loaded calcite samples (initial concentration = 10,000 mg/L of $\text{Zn}(\text{NO}_3)_2$) at contact periods ranging from 1 h up to 1 week. The gradual overgrowth of hydrozincite features is evident from the figure, which shows also a paralleling gradual decrease in the intensity of calcite features. This observation is inline with the reported hindrance in calcite crystallization in favor of hydrozincite formation in Ca^{2+} - and CO_3^{2-} -bearing solutions exposed to large amounts of Zn^{2+} ions [17].

These results were also supported by the EDS analysis. Fig. 6 provides typical EDS spectra that show the gradual progress of Zn signals after loading. SEM images of pure calcite and Zn-loaded calcite are also provided in the same figure. As illustrated by Table 4, the EDS quantification, as atom percentage, have shown that, within the studied experimental conditions, the enrichment of calcite by Zn is particularly fast during the first 24 h. The uptake then seems to proceed at a smaller rate during the following days (or even weeks). It is interesting to see that the initial fast uptake of Zn^{2+} was not paralleled by a fast overgrowth of zinc carbonate species even at oversaturation conditions, indicating slow overgrowth kinetics. It might be proposed that Zn^{2+} ions, in the earlier hours of contact, are fixed by ion exchange (or attached to the crystal imperfections and/or surface groups of calcite) and later undergo a slower process of recrystallization leading to the development of the hydrozincite phase on a time scale from days or weeks, depending on the reaction conditions. Thus, it is essential to take the kinetic factor

into consideration when reporting the sorption mechanism of Zn^{2+} on calcite.

The effect of Zn^{2+} retention on the structure of calcite was also followed using FTIR spectroscopy. The incorporation of Zn^{2+} is expected to affect the initial D_{3h} symmetry of carbonate group in calcite due to the difference in size between Zn^{2+} (0.74 Å) and Ca^{2+} (0.99 Å). In an earlier study performed using surface-extended X-ray absorption fine structure (SEXAFS), it was concluded that substitution of Zn^{2+} for Ca^{2+} within calcite leads to structural relaxation of the coordinating carbonate ligands in response to the smaller size of Zn^{2+} [18]. In the Zn–calcite samples, where no hydrozincite overgrowth was detected, the main effect of Zn uptake was a slight activation of the initially inactive symmetric stretching band (1056 cm^{-1}) as a result of the change in the D_{3h} symmetry of calcite. On the other hand, the overgrowth of hydrozincite caused the development of new bands that differ seriously from the initial vibrational bands of calcite. Fig. 7 provides the FTIR spectra of calcite prior to and after Zn^{2+} loading at the highest studied concentration of 10,000 mg/L $\text{Zn}(\text{NO}_3)_2$. The changes in the FTIR spectra include a split in the asymmetric vibrational band of the mineral occurring initially at 1443 cm^{-1} , activation of the initially inactive symmetric stretching feature located at 1056 cm^{-1} , development of a hydroxide stretching feature at 3344 cm^{-1} , possibly arising from the hydroxide groups in the hydrozincite structure, and splitting of the in-plane and out-of-plane bending modes occurring at 716 and 876 cm^{-1} , respectively.

4. Conclusion

Calcite possesses a larger sorption capacity for Zn^{2+} compared to kaolinite and clinoptilolite. Hence, calcite presence as a soil component is expected to correlate positively with the sorption properties of soil, in particular in the neutral and alkaline media. In the calcite–kaolinite and calcite–clinoptilolite mixtures, the efficiency of calcite becomes clearer at higher loadings, where the sorption process becomes predominantly controlled by the amount of calcite in the mixtures. At high initial Zn^{2+} concentrations, the sorption mechanism on calcite seems to start via an initial ion exchange step (time scale is hours) followed by a slower process that leads to overgrowth of hydrozincite (time scale ranges from days to weeks).

Acknowledgments

This work was sponsored through the research fund 2003 İYTE 03. The authors also thank the Center of Materials Research at IZTECH for their help in the XRPD and SEM/EDS measurements.

References

- [1] I. Montilla, M.A. Parra, J. Torrent, *Plant Soil* 257 (2003) 227.
- [2] U. Hoffmann, S.L.S. Stipp, *Geochim. Cosmochim. Acta* 65 (2001) 4131.
- [3] J. Ikhsan, B.B. Johnson, J.D. Wells, *J. Colloid Interface Sci.* 217 (1999) 403.
- [4] A.K. Darban, A. Foriero, R.N. Yong, *Eng. Geol.* 57 (2000) 81.
- [5] A. Cincotti, N. Lai, R. Orrù, G. Cao, *Chem. Eng. J.* 84 (2001) 275.
- [6] V. Badillo-Almaraz, P. Trocellier, I. Dávila-Rangel, *Nucl. Instrum. Methods B* 210 (2003) 424.
- [7] J. Perić, M. Trgo, N.V. Medvidović, *Water Res.* 38 (2004) 1893.
- [8] E.J. Elzinga, R.J. Reeder, *Geochim. Cosmochim. Acta* 66 (2002) 3943.
- [9] L. Cheng, N.C. Sturchio, J.C. Woicik, K.M. Kemner, P.F. Lyman, M.J. Bedzyk, *Surf. Sci.* 415 (1998) L976.
- [10] D. Wenming, G. Zhijun, D. Jinzhou, Z. Liying, T. Zuyi, *Appl. Radiat. Isotopes* 54 (2001) 371.
- [11] L.M. Ottosen, H.K. Hansen, A.B. Ribeiro, A. Villumsen, *J. Hazard. Mater.* 85 (2001) 291.
- [12] J.C. Echeverría, M.T. Morera, C. Mazkiarán, J.J. Garrido, *Environ. Pollut.* 101 (1998) 275.
- [13] M.E. Mesquita, J.M. Vieira e Silva, *Geoderma* 69 (1996) 137.
- [14] W. Stumm, J.J. Morgan, *Aquatic Chemistry*, Wiley, New York, 1996, p. 296.
- [15] N. Xu, M.F. Hochella Jr., G.E. Brown Jr., G.A. Parks, *Geochim. Cosmochim. Acta* 60 (1996) 2801.
- [16] A. García-Sánchez, E. Álvarez-Ayuso, *Miner. Eng.* 15 (2002) 539.
- [17] S.J. Freij, A. Godelitsas, A. Putnis, *J. Cryst. Growth* 273 (2005) 535.
- [18] L. Cheng, N.C. Sturchio, J.C. Woicik, K.M. Kemner, P.F. Lyman, M.J. Bedzyk, *Surf. Sci.* 415 (1998) L976.